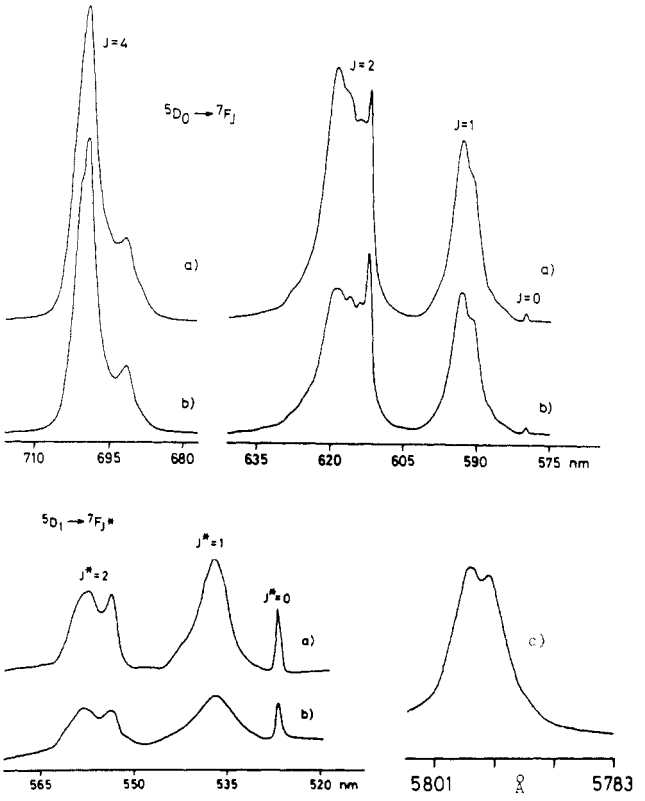

Figure 9. Emission spectra of anhydrous Me_2SO solutions with $Eu(NO_3)_3$ of the following concentrations (λ_{exc} = 394 nm): (a) 0.1 M; (b) 0.01 M; (c) 0.1 M, $^5D_0 \rightarrow {}^7F_0$ transition.

$(NO_3)(Me_2SO)_y]^{2+}$ and $[Eu(Me_2SO)_n]^{3+}$, in the approximate ratio 1:6.5. The number of coordinated Me_2SO molecules could not be determined with sufficient accuracy from IR data.[21] However, if we refer to the above discussion, n is likely to be equal to 9 and y to 7.

The inner-sphere interaction of the nitrate ion is further evidenced by conductivity and fluorescence data (Figure 9). The molar conductivities of $Eu(NO_3)_3$ solutions 10^{-4}, 5×10^{-4}, 10^{-3}, 2×10^{-3}, and 4×10^{-3} M in Me_2SO are equal to 115, 107, 102, 101, and 73 Ω^{-1} mol^{-1} cm^2, respectively, at 25 °C. These values are slightly smaller than the conductivities found for the perchlorate solutions. The emission spectrum of a 0.01 M solution (lifetime 1.40 ms) is similar to the spectra of the perchlorate solutions, whereas the spectrum of 0.1 M $Eu(NO_3)_3$ (lifetime 1.35 ms) displays substantial intensity changes (Figure 9). The $^5D_0 \rightarrow {}^7F_0$ transition is comprised of two components, at 579.55 and 579.15 nm, corresponding to the two above-mentioned solvated species. It is interesting to note its large intensity variation when Me_2SO molecules are removed from the first coordination sphere of the Eu^{3+} ion. For solutions 0.05 M in Eu^{3+}, $^7F_0/^7F_1$ amounts to 0.3, 0.9, 1.2, 1.4, and 10% for $[Eu(Me_2SO)_9]^{3+}$, $[Eu(NO_3)(Me_2SO)_y]^{2+}$, $[Eu(NO_3)_2(Me_2SO)_x]^{+}$, $Eu(NO_3)_3(Me_2SO)_3$, and $Eu(NO_3)_3(CH_3CN)_3$, respectively.

The quantum yield of the $^5D_0$ emission upon excitation to the $^5L_6$ level for $Eu(NO_3)_3$ 0.1 M in Me_2SO amounts to 20.4%, as measured by taking $Eu(NO_3)_3 \cdot 6H_2O$ 0.1 M in CH_3OH as standard (Q = 5%[22]).

The apparent equilibrium ratio $[Eu(NO_3)(Me_2SO)_7^{2+}]:[Eu(Me_2SO)_9^{3+}]\cdot[NO_3^-]$ can be estimated to 1.1 ± 0.2 M^{-1} for a $Eu(NO_3)_3$ solution 0.05 M in Me_2SO. The corresponding value we have reported for aqueous solutions was 0.3 ± 0.1 M^{-1}. With the assumption that each nitrate displaces two solvent molecules, these ratios have to be multiplied by the square of the solvent concentrations, $[S]^2$, to obtain the apparent constants, K_{app}, of the equilibria

$$[EuS_n]^{3+} + NO_3^- \rightleftarrows [Eu(NO_3)S_{n-2}]^{2+} + 2S$$

The K_{app} values are approximately equal to 200 and 900 M for Me_2SO and H_2O, respectively, which reflects the stronger affinity of the europium ion for the dimethyl sulfoxide molecules.

Acknowledgment. Financial support from the Swiss National Science Foundation (Project 2.844-0.80) is gratefully acknowledged. We thank Ms. Angela Sottile for technical assistance and the Fondation Herbette (Lausanne) for the gift of the pulsed laser.

Registry No. Eu, 7440-53-1; Me_2SO, 67-68-5; $Eu(NO_3)_3$, 10138-01-9; $Eu(ClO_4)_3$, 13537-22-9.

Supplementary Material Available: Listings of emission intensities and lifetimes of 0.05 M $Eu(ClO_4)_3 \cdot R(Me_2SO)$ in CH_3CN ($0 \le R \le 20.3$) (Table S1), deconvolutions of IR spectra of the above-mentioned solutions (1000–1100 cm^{-1}) (Table S2), and emission intensities and lifetimes of 0.05 M $Eu(NO_3)_3 \cdot R(Me_2SO)$ in CH_3CN ($4 \le R \le 275$) (Table S3) (3 pages). Ordering information is given on any current masthead page.

(21) The numbers of y and z could not be accurately determined from the IR data because of the presence of large absorptions arising from bulk Me_2SO molecules.

(22) Dawson, W. R.; Kropp, J. L. *J. Opt. Soc. Am.* **1965**, *55*, 822.

Contribution from the Laboratoire de Chimie du Solide du CNRS, Université de Bordeaux I, 33405 Talence Cedex, France

Magnetic and Mössbauer Resonance Investigations of the Weak Ferrimagnet $Fe_2(MoO_4)_3$

Z. JIRAK, R. SALMON,* L. FOURNES, F. MENIL, and P. HAGENMULLER

Received November 10, 1981

Magnetic and Mössbauer resonance measurements have shown that $Fe_2(MoO_4)_3$ exhibits below an ordering temperature of about 13 K a weak ferrimagnetism due to incomplete compensation of the magnetization of antiferromagnetically coupled sublattices. From the analysis of the exchange links Fe–O–Mo–O–Fe and from the Mössbauer resonance spectra a possible arrangement of the spins has been deduced.

Introduction

The catalytic properties of $Fe_2(MoO_4)_3$ are well-known in the process of selective oxidation of methanol to formaldehyde. Ferric molybdate is also present in multicomponent catalysts used for the ammoxidation of propene to acrylonitrile and for the oxidation of propene to acrolein.

Numerous studies have been carried out in order to try to improve the activity of these catalysts.[1-8] However, the few

0020-1669/82/1321-4218$01.25/0

works devoted to pure $Fe_2(MoO_4)_3$ deal mainly with its crystal structure.[9-12] Obviously the knowledge of other physical properties of this material is required to explain its catalytic behavior. For this purpose, magnetic and Mössbauer resonance investigations have been undertaken.

Before our results are reported and discussed, the crystal structure of ferric molybdate will be briefly recalled. Ferric molybdate occurs in two crystalline forms: monoclinic $Fe_2(MoO_4)_3$ transforms reversibly at 499 °C into an orthorhombic variety.[13] Recent studies of the room-temperature single-crystal X-ray structure of the monoclinic form, which is only concerned in this paper, differ in the determination of the space group. According to Rapposch et al.,[12] the space group is $P2_1$, whereas Chen[11] refined the structure with the centrosymmetric group $P2_1/a$. The failure to observe a second harmonic signal supports the centrosymmetric group. Therefore, we shall refer here to the structure reported by Chen. We note, however, that topologically both structures are very similar. They consist of (FeO_6) octahedra sharing corners with (MoO_4) tetrahedra. All the octahedra are isolated from each other and so are the tetrahedra. Each oxygen is linked only to one iron and to one molybdenum. Thus, the structure of ferric molybdate exhibits features analogous to those of ferric sulfate, $Fe_2(SO_4)_3$,[14,15] or sodium iron phosphate, $Na_3Fe_2(PO_4)_3$,[16] as far as the three-dimensional network of (FeO_6) octahedra and of (XO_4) tetrahedra is concerned.

Experimental Section

Ferric molybdate was prepared according to the method proposed by Trifiro et al.[17] In a typical way 360 cm^3 of a 0.0183 M solution of ammonium heptamolybdate was acidified by nitric acid until pH 1.8. Then 90 cm^3 of 0.33 M solution of ferric nitrate was added under stirring. The precipitate obtained was aged during 4 h at 80 °C under stirring, then filtered, washed with acidified water, dried 15 h at 200 °C, and finally calcinated at 480 °C. The resulting powder was yellow-green. Its X-ray diffraction pattern was indexed with the following parameters: a = 15.73 Å, b = 9.23 Å, c = 18.216 Å, and β = 125.2°, in agreement with previously reported results. Moreover, an X-ray investigation at 4.2 K revealed that no structural modification occurred at low temperature except the usual decrease of the lattice parameters whose values at 4.2 K are a = 15.60 Å, b = 9.18 Å, c = 18.00 Å, and β = 125.0°.

Iron and molybdenum contents were determined by atomic absorption: 18.7 ± 0.1 wt % for Fe (calcd 18.9) and 48.8 ± 0.2 wt % for Mo (calcd 48.7).

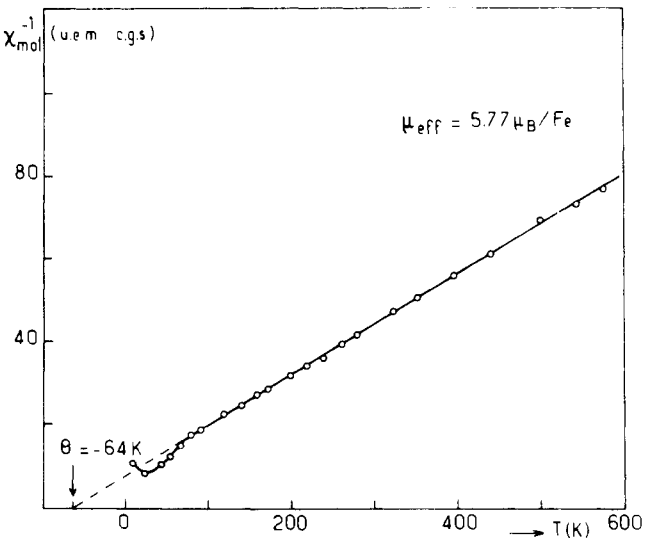

Figure 1. Inverse molar magnetic susceptibility of $Fe_2(MoO_4)_3$ vs. temperature.

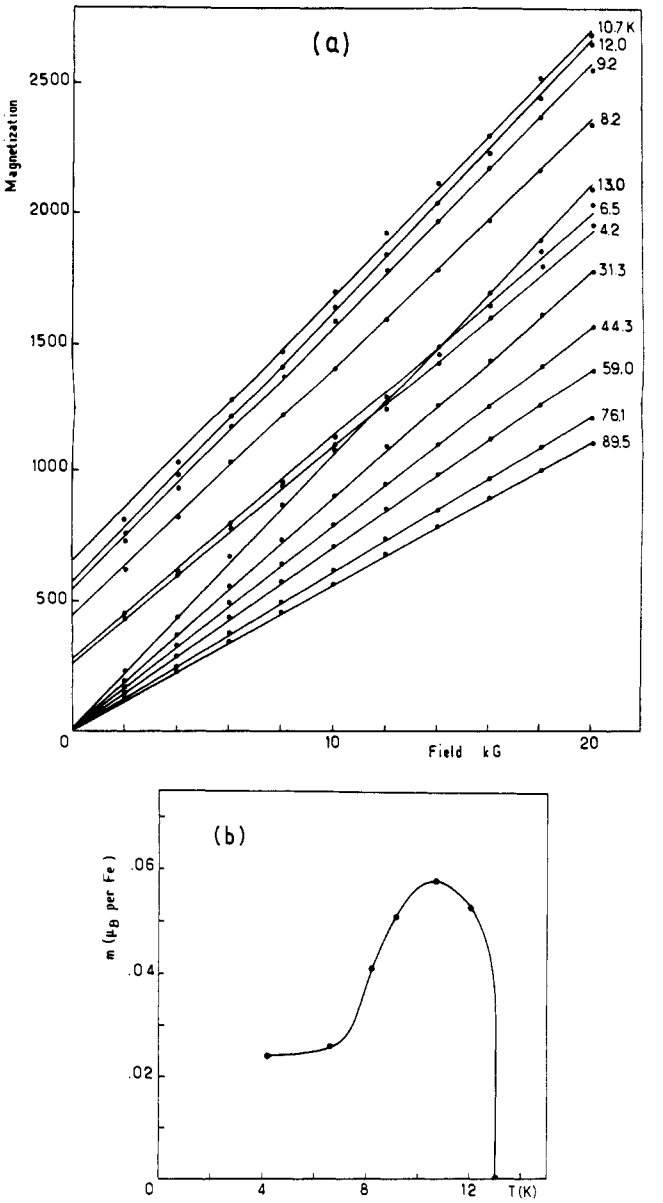

Figure 2. (a) Magnetization of ferric molybdate as a function of applied field at various temperatures. (b) Temperature dependence of spontaneous magnetization of $Fe_2(MoO_4)_3$.

(1) G. Fagherazzi and N. Pernicone, *J. Catal.*, **16**, 321 (1970).
(2) G. Alessandrini, L. Cairati, P. Forzatti, P. L. Villa, and F. Trifiro, *J. Less-Common Met.*, **54**, 373 (1977).
(3) F. Trifiro, V. de Vecchi, and I. Pasquon, *J. Catal.*, **15**, 8 (1966).
(4) N. Pernicone, *J. Less-Common Met.*, **36**, 289 (1974).
(5) P. L. Villa, A. Szabo, F. Trifiro, and M. Carbucicchio, *J. Catal.*, **47**, 122 (1977).
(6) F. Figueras, C. Pralus, M. Perrin, and A. J. Renouprez, *C. R. Hebd. Seances Acad. Sci., Ser. C*, **282**, 373 (1976).
(7) P. Courty, H. Ajot, and B. Delmon, *C. R. Hebd. Seances Acad. Sci., Ser. C*, **276**, 1147 (1973).
(8) M. Carbucicchio and F. Trifiro, *J. Catal.*, **45**, 77 (1976).
(9) L. M. Plyasova, R. F. Klevtsova, S. V. Borisov, and L. M. Kefeli, *Sov. Phys.—Dokl. (Engl. Transl.)*, **11**, 189 (1966).
(10) L. M. Plyasova, S. V. Borisov, and N. V. Belov, *Sov. Phys.—Crystallogr. (Engl. Transl.)*, **12**, 25 (1967).
(11) H.-Y. Chen, *Mater. Res. Bull.*, **14**, 1583 (1979).
(12) M. H. Rapposch, J. B. Anderson, and E. Kostiner, *Inorg. Chem.*, **19**, 3531 (1980).
(13) A. W. Sleight and L. H. Brixner, *J. Solid State Chem.*, **7**, 172 (1973).
(14) P. B. Moore and T. Araki, *Neues Jahrb. Mineral., Abh.*, **121**, 208 (1974).
(15) P. C. Christidis and P. J. Rentzeperis, *Z. Kristallogr.*, **144**, 341 (1976).
(16) C. Delmas, R. Olazcuaga, F. Cherkaoui, R. Brochu, and G. Le Flem, *C. R. Hebd. Seances Acad. Sci., Ser. C*, **287**, 169 (1978).
(17) F. Trifiro, L. Cairati, and P. L. Villa, Italian Patent 25 545 (1974), p A74.

Table I. Electric Field Gradient Tensor and Calculated Quadrupole Splitting Δ

site[a]	principal axes	principal values, 10^{24} cm^{-3}			$\eta = (V_{yy} - V_{xx})/V_{zz}$	Δ_{calcd},[b] mm·s^{-1}
		V_{xx}/e	V_{yy}/e	V_{zz}/e		
1	$X = 0.74x + 0.10y - 0.67z$ $Y = 0.01x + 0.99y + 0.16z$ $Z = 0.68x - 0.12y + 0.73z$	−0.066	−0.021	0.087	0.52	0.30
2	$X = 0.79x + 0.31y + 0.53z$ $Y = -0.25x + 0.95y - 0.19z$ $Z = -0.56x + 0.02y + 0.83z$	0.077	0.001	−0.078	0.96	0.29
3	$X = 0.44x + 0.76y - 0.48z$ $Y = 0.14x + 0.47y + 0.87z$ $Z = 0.89x - 0.45y + 0.09z$	−0.071	−0.021	0.092	0.54	0.32
4	$X = 0.84x + 0.02y + 0.55z$ $Y = 0.00x + 1.00y - 0.04z$ $Z = -0.55x + 0.03y + 0.84z$	0.036	0.075	−0.111	0.36	0.37

[a] The positions on the monoclinic axes *a*, *b*, *c* are as follows. Site 1: [0.1193, 0.4651, 0.6810]. Site 2: [0.1300, 0.9593, 0.9552]. Site 3: [0.1191, 0.4738, 0.1852]. Site 4: [0.1059, 0.9830, 0.4159]. [b] $\Delta_{calcd} = (1 - \gamma_\infty)(e^2QV_{zz}/2)(1 + \eta^2/3)^{1/2}$, $\gamma_\infty = -10$, $eQ = 0.2 \times 10^{-24}$ cm^2.

Magnetization data in the temperature range 4.2–90 K were obtained with a Foner type magnetometer (maximum applied field 20 kG). At higher temperatures, the magnetic susceptibility measurements were performed with a Faraday balance.

The Mössbauer spectra were obtained from 4.2 to 293 K with a classical device described elsewhere.[18] The samples contained less than 10 mg·cm^{-2} of natural iron, a concentration for which line broadening due to thickness effects is usually not noticeable.

Magnetic Investigation

The temperature dependence of the inverse molar magnetic susceptibility of $Fe_2(MoO_4)_3$ shown in Figure 1 is typical of antiferromagnets. The effective moment per iron atom worked out from the linear part of the curve is equal to 5.77 μ_B, in fair agreement with the theoretical value (5.92 μ_B). The paramagnetic Curie temperature $\Theta = -64$ K is very close to that reported by Rapposch et al. (−62.7 K).

The magnetization curves vs. applied field (Figure 2a) show the appearance of a spontaneous magnetization below 13 K, which was taken as the Néel temperature of the material. The weak ferromagnetic moment obtained from the extrapolation of the curves in Figure 2a to zero applied field increases to a maximum value of 0.057 μ_B per iron atom at about 10 K and decreases again at lower temperatures (Figure 2b).

Mössbauer Resonance Study

The Mössbauer spectra in the paramagnetic state are typical of high-spin ferric ions (Figure 3). They were fitted to a doublet of Lorentzians of width $\Gamma = 0.28$ mm·s^{-1} with a quadrupole splitting $\Delta = 0.20 \pm 0.01$ mm·s^{-1}. The isomer shifts δ at 293 and 13 K are 0.41 ± 0.01 and 0.52 ± 0.01 mm·s^{-1} relative to α-Fe, respectively. The room-temperature parameters are very similar to those reported previously.[19,20]

When the isomer shift values of $Fe_2(MoO_4)_3$ are compared to those of $Na_3Fe_2(PO_4)_3$[21] and $Fe_2(SO_4)_3$,[22-24] which have related structures, a significant increase is observed in the sense $\delta_{molybd} < \delta_{phosph} < \delta_{sulf}$ (for example, at 293 K $\delta_{phosph} = 0.45$ mm·s^{-1} and $\delta_{sulf} = 0.49$ mm·s^{-1}). This trend likely corresponds to an increase of the ionic character of the Fe–O bond as a consequence of increasing covalency of the antagonistic bond

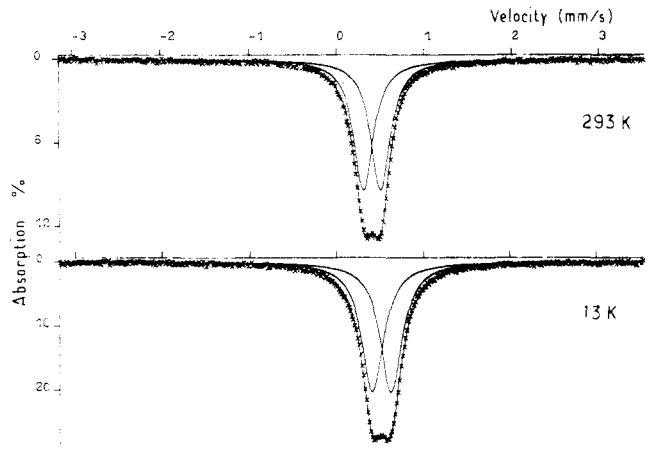

Figure 3. Mössbauer resonance spectra of $Fe_2(MoO_4)_3$ in the paramagnetic state.

X–O from molybdate to sulfate (for the three compounds, the temperature dependences of the isomer shifts are similar, which indicates comparable values of the Debye temperatures and therefore enables to neglect the effect of second-order shift in the comparison of the isomer shifts at room temperature).

The rather small quadrupole splitting value is indicative of only minor distortions of the (FeO_6) octahedra. From structural data of Chen,[11] the electric field gradient tensor has been calculated in the approximation of point charges 2−, 3+, and 6+ for O, Fe, and Mo ions, respectively. The lattice sum results within a sphere of 40-Å radius are summarized in Table I by using an orthogonal coordination system *x*, *y*, *z* defined as $x \| b$, $y \| c$, $z \| u$ (*u* is perpendicular to the *bc* plane). It turns out from the computation that the values of Δ_{calcd} do not differ much for the various sites, in agreement with the relative narrowness of the doublet lines. The ~50% discrepancy between calculated values of Δ and the observed quadrupole splitting is likely due to the inadequacy of the adopted model, which assumes integral charges for the ions and/or to small deviations of the real structure from the referred one. It is worthwhile noticing that such differences between calculated and observed values of Δ are not unusual when this type of procedure is used.

In the magnetically ordered state the Mössbauer spectra consist apparently of two sextuplets with practically zero quadrupole perturbations, the most intense (sextuplet α) corresponding to the smaller hyperfine field (Figure 4). Moreover, the outer lines of sextuplet α are very broad ($\Gamma \simeq 0.6$ mm·s^{-1}) and show non-Lorentzian features. Therefore, in order to fit the spectra with acceptable χ^2 values ($\chi^2 \simeq 2$)

(18) F. Ménil, M. Pezat, and B. Tanguy, *C. R. Hebd. Seances Acad. Sci., Ser. C*, **281**, 849 (1975).
(19) C. L. Herzenberg and D. L. Riley, *J. Phys. Chem. Solids*, **30**, 2108 (1969).
(20) R. R. Zakirov, G. M. Bartenev, and A. D. Tsyganov, *J. Struct. Chem. (Engl. Transl.)*, **16**, 568 (1975).
(21) D. Beltrán-Porter, R. Olazcuaga, L. Fournes, F. Menil, and G. Le Flem, *Rev. Phys. Appl.*, **15**, 1155 (1980).
(22) Y. Haven and R. E. Noftle, *J. Chem. Phys.*, **67**, 2825 (1977).
(23) G. J. Long, G. Longworth, P. Battle, A. K. Cheetham, R. V. Thundathil, and D. Beveridge, *Inorg. Chem.*, **18**, 624 (1979).
(24) J. W. Culvahouse, *J. Magnetism Magn. Mater.*, **21**, 133 (1980).

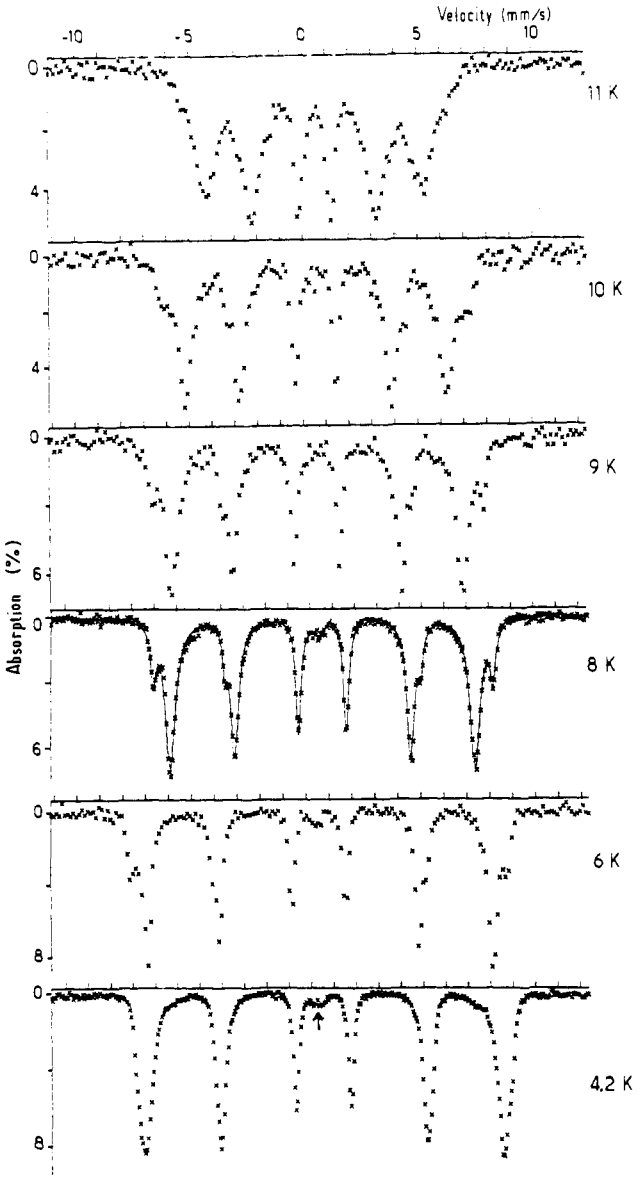

Figure 4. Mössbauer resonance spectra of $Fe_2(MoO_4)_3$ below ordering temperature $T_N \simeq 13$ K. The arrow in the spectrum at 4.2 K corresponds to an unidentified paramagnetic impurity with a content less than 1%.

and to get a relevant value of the area ratio between both sextuplets, we employed a computer program using quasi-continuous distributions of hyperfine fields for each sextuplet.[25] At each temperature in the 6–10 K range a ratio of about 3:1 was found for the area of sextuplet α to that of sextuplet β (at 4.2 K and above 10 K a precise determination of the ratio is difficult because of greater overlapping of the sextuplets). From the area ratio, it was deduced that sextuplet β corresponded to one of the four iron sites in the structure refined by Chen[11] and sextuplet α to the three others.

The temperature dependence of the averaged hyperfine fields for sextuplets α and β is reported in Figure 5a. The extrapolation of the curves to zero hyperfine field yields a value of 12 K for the Néel temperature, in very good agreement with the magnetization measurements. Figure 5b shows the difference between the hyperfine fields as a function of temperature. This curve exhibits a trend analogous to that observed for magnetization vs. T (Figure 2b). It is worth emphasizing that such a behavior was already observed for $Fe_2(SO_4)_3$[23] and was attributed to a "weak ferrimagnetism"

(25) G. Le Caer and J. M. Dubois, *J. Phys. E*, **12**, 1083 (1979).

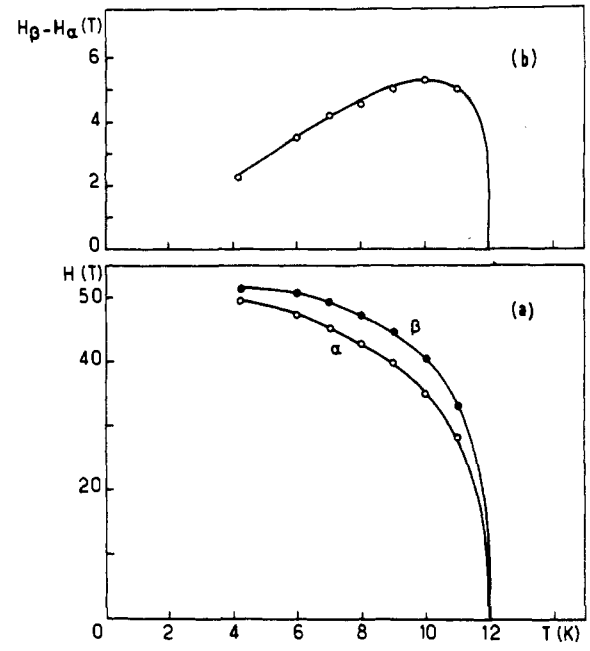

Figure 5. Plots of the averaged hyperfine fields for sextuplets α and β (a) and of the difference between these fields (b) as functions of temperature.

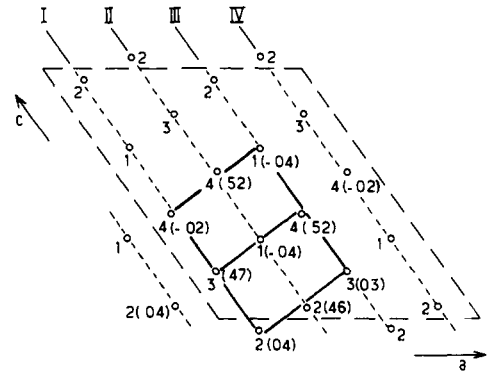

Figure 6. Iron positions in the $Fe_2(MoO_4)_3$ lattice projected along the monoclinic b axis (b coordinates of some iron atoms are given in parentheses).

arising from incomplete compensation of antiferromagnetically coupled sublattices.[24] In order to find out whether a similar explanation can be applied to ferric molybdate, we shall now discuss possible magnetic arrangements.

Proposition of a Magnetic Model

The iron cations in four inequivalent sites of the $Fe_2(MoO_4)_3$ structure are arranged approximately in a distorted body-centered cubic lattice. Such a pseudocubic cell viewed along its face diagonal is marked by heavy lines in Figure 6. Each iron atom has eight nearest iron neighbors and six next-nearest iron neighbors. Six (MoO_4) tetrahedra around each iron provide eighteen exchange links (Fe–O–Mo–O-Fe) to the fourteen neighbors. There are six links to the next-nearest neighbors and twelve links to the nearest neighbors, half of them being connected by double links. In order to make the following discussion easier, it is convenient to represent the structure by sheets parallel to the bc plane (see Figure 6). Thus, all the links between nearest neighbors in I–II and III–IV interlayers are single and those in II–III and IV–I interlayers are double.

Supposing that the magnetic arrangement keeps the dimension of the elementary cell, we can analyze possible spin ordering. For every crystallographically distinct iron site there is just one position per unit cell in each I, II, III, IV sheet.

Table II. Minimum-Energy Magnetic Structures

structure	mode	spin orientation in site no.[a] 1	2	3	4
i	F_aF_c or F_b	+	−	+	−
ii	A_aA_c or A_b	+	−	+	−
iii	A_aA_c or A_b	+	+	+	+

[a] For positions see footnote *a* in Table I.

If we label accordingly four equivalent positions for each site, the spin components in the *a*, *b*, *c* directions can be expressed by using their four linear combinations:

$$F = S_I + S_{II} + S_{III} + S_{IV}$$
$$A = S_I - S_{II} + S_{III} - S_{IV}$$
$$C = S_I + S_{II} - S_{III} - S_{IV}$$
$$G = S_I - S_{II} - S_{III} + S_{IV}$$

(here the indices specifying the type of site—1, 2, 3, 4—and the direction—*a*, *b*, *c*—are omitted).

In the symmetry operation each mode is transformed according to certain one-dimensional representation of the space group $P2_1/a$. In the ground state the spin components in all directions and in all inequivalent sites must belong to the same representation. This follows from the requirement of invariancy of the exchange Hamiltonian.[26] The analysis shows that within one iron site the possible couplings are $G_aF_bG_c$, $A_aC_bA_c$, $F_aG_bF_c$, and $C_aA_bC_c$. The consequence is that, if we restrict ourselves only to the collinear structures, the arrangement can be of type F, A, C, or G and the spins can lie either in the *ac* plane or along the *b* axis. The orientation of the spins with respect to the spins of other iron sites is actually controlled by the strength of exchange interactions between the sites. We suppose that all interactions via Fe–O–Mo–O–Fe links are antiferromagnetic and additive.

If it is assumed that the strengths of all exchange interactions are similar, all four iron sites are equivalent with regard to the 18 exchange links with 14 neighbors. The analysis over 44 possible collinear arrangements shows that the minimum exchange energy (12 links with antiferromagnetic coupling and 6 links with ferromagnetic coupling) can be achieved by three types of ordering. The corresponding magnetic structures are shown in Figure 7. In Table II they are specified by the mode and by the orientation of the spins for different sites in sheet I. Magnetic structure i is of compensated ferrimagnet type, whereas structures ii and iii are pure antiferromagnets.

The weak ferromagnetic component determined for $Fe_2(MoO_4)_3$ by magnetization measurements (see Figure 2) can be explained either by a slight canting (weak ferromagnetism) or by an incomplete compensation of the collinear arrangement (weak ferrimagnetism). Canting can arise only in the structures of mode G and is incompatible therefore with the configurations suggested in Table II. It also does not explain the different hyperfine fields observed by Mössbauer measurements in a consistent way. On the other hand, the weak ferrimagnetic moment which can arise in magnetic structure i may explain satisfactorily both magnetization and Mössbauer results. In this structure the magnetic moments in two sites are aligned in one sense and in the other two sites in the opposite sense. At zero temperature their values will be nearly the same ($\sim 5\mu_B$ per Fe^{3+} ion), leading to approximately zero net magnetization. At temperatures closer to T_N the temperature-averaged moments differ because of the so far neglected differences in exchange interactions.

In view of the above results, it is now interesting to discuss the quantitative features of the curves in Figures 2b and 5b. It is usually admitted that the hyperfine field H is proportional

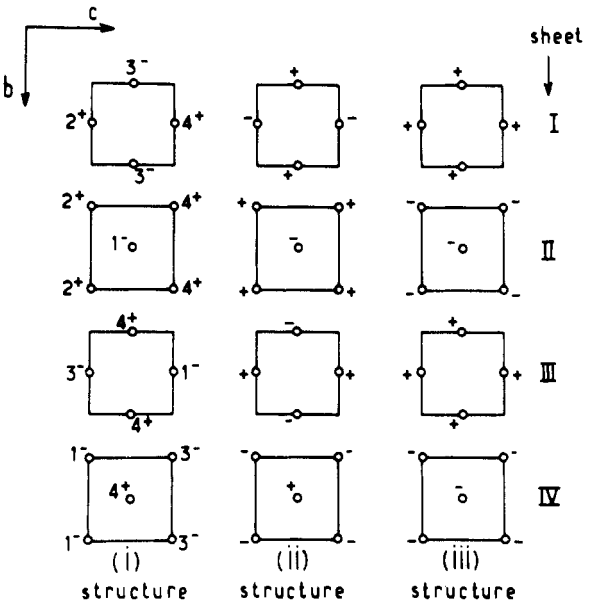

Figure 7. Magnetic structures i–iii (iron positions are represented in a body-centered cubic lattice; site numbers are valid for the cell described in Figure 6).

to the sublattice magnetization at all temperatures. As we stated previously, subscript α will refer to the three sublattices corresponding to the three crystallographic sites with close values of H (average value H_α) and subscript β to the remaining site. Therefore, one can write

$$H_\alpha(T) = k_\alpha(\mu_\alpha(T)) \qquad H_\beta(T) = k_\beta(\mu_\beta(T))$$

where μ is the sublattice magnetization per iron atom and k the proportionality constant.

At 0 K, it is well-known that the magnetic moments of Fe^{3+} are always very close to 5 μ_B. Consequently, one may assume

$$\mu_\alpha(0) = \mu_\beta(0) = \mu(0) = 5\ \mu_B$$

Defining $\Delta H(T) = H_\beta(T) - H_\alpha(T)$ and $\Delta\mu(T) = \mu_\beta(T) - \mu_\alpha(T)$, one easily finds

$$\Delta H(T) = \frac{\Delta\mu(T)}{\mu(0)} H_\beta(0) + \frac{\mu_\alpha(T)}{\mu(0)} \Delta H(0)$$

In the case of $Fe_2(SO_4)_3$, $\Delta H(0) \to 0$ and the above relationship reduces to

$$\Delta H(T) \simeq \frac{\Delta\mu(T)}{\mu(0)} H(0)$$

It is found that the latter relationship is roughly verified when the experimental data reported in ref 23 are used.

As for $Fe_2(MoO_4)_3$, the experimental values of $[\Delta\mu(T)/\mu(0)]H(0)$ are about one-half or one-third of those of $\Delta H(T)$, according to the selected value of T. This result would imply, contrary to the case of ferric sulfate, different saturation values for H_α and H_β ($\Delta H(0) \neq 0$). It is important to note that the experimental values of $\Delta\mu(T)$ were obtained by multiplying the experimental spontaneous magnetizations per iron atom by 2 in the case of $Fe_2(SO_4)_3$ and by 4 in the case of $Fe_2(MoO_4)_3$ in order to take into account the different number of sublattices in both compounds.

It is well-known that the Mössbauer spectra in the magnetically ordered state give some possibility to derive the spin direction relative to the EFG tensor axes. The calculation can be based on sextuplet β, which corresponds to a single site. As can be deduced from the largest hyperfine field for sextuplet β, the relevant site should be that with the strongest Fe–O–Mo–O–Fe links. Generally, these are all the stronger, the

(26) E. Bertaut, *J. Phys. (Orsay, Fr.)*, **35**, 659 (1974).

Table III. Average Values for the Exchange Links Corresponding to Different Iron Sites in $Fe_2(MoO_4)_3$

	site no.			
	1	2	3	4
pathway, Å	7.488	7.497	7.486	7.475
Fe-O-Mo, deg	149.7	147.5	150.7	153.2

shorter is the total pathway, the closer is the O–Mo–O angle to that of a regular tetrahedron, and the closer are the Fe–O–Mo angles to 180°. Because the distortions of (FeO_6) octahedra and (MoO_4) tetrahedra are very small, the exchange interaction is likely to depend mostly on the Fe–O–Mo angles, which vary in the range 133.2–167.6°. It appears from the comparison of mean angles and lengths of pathways (see Table III) that site 4 is likely to correspond to sextuplet β. From the value for quadrupole splitting in the paramagnetic state $\Delta_{obsd} = 0.20$ mm·s^{-1}, $\eta_{calcd} = 0.36$, and the orientation of the principal axes of the EFG tensor for site 4 (Table I), the quadrupole perturbation has been calculated for possible orientations of the magnetic axis and compared with the experimental value $\epsilon = 0.00 \pm 0.02$ mm·s^{-1}. The results suggest that the magnetic moments lie in the *ac* plane, making an angle of 37–58 or 122–143° with the *c* axis as the most plausible solution.

It is worth emphasizing that the latter result relies on many hypotheses and that a neutron diffraction investigation should be undertaken in order to determine the magnetic structure unambiguously.

Acknowledgment. The present work has been performed with the financial support of Rhône-Poulenc SA. The authors wish to thank B. Chevalier, who carried out the X-ray diffraction experiments at 4.2 K and Professor R. Georges for helpful discussions.

Registry No. $Fe_2Mo_3O_{12}$, 13769-81-8.

Contribution from the Inorganic Chemistry Laboratory, Oxford University, Oxford OX1 3QR, England, the Chemical Crystallography Laboratory, Oxford University, Oxford OX1 3PD, England, the Department of Chemistry, University of Missouri—Rolla, Rolla, Missouri 65401, and the Nuclear Physics Division, Atomic Energy Research Establishment, Harwell, Didcot OX11 0RA, England

Study of the Magnetic Properties of Iron(III) Molybdate, by Susceptibility, Mössbauer, and Neutron Diffraction Techniques

PETER D. BATTLE,*[1a] ANTHONY K. CHEETHAM,[1b] GARY J. LONG,*[1c,d] and GEOFFREY LONGWORTH[1d]

Received November 23, 1981

A powder neutron diffraction study and subsequent line-profile analysis of the magnetic structure of iron(III) molybdate at 2 K indicate that it is a four-sublattice antiferromagnet containing four crystallographically distinct iron atoms in the space group $P2_1/a$ (*b* unique). The results also confirm that the 2 K nuclear structure is the same as that found at room temperature by single-crystal X-ray diffraction. An analysis of covalency in iron(III) molybdate reveals a higher degree of covalency ($A_\sigma^2 + 2A_\pi^2 + A_s^2 = 9.15\%$) in the iron(III) to oxygen bonds than is found in the structurally related iron(III) sulfate (6.1%). A Mössbauer-effect study indicates that, at 11.8 K and above, iron(III) molybdate is paramagnetic with parameters typical of an octahedral high-spin iron(III) compound. Between 11.72 and 11.59 K both ordered and paramagnetic phases coexist. Below 11.72 K the Mössbauer spectrum shows the presence of spontaneous magnetic ordering with four inequivalent magnetic hyperfine fields. On three of the iron sites, the hyperfine fields are rather similar while the fourth site exhibits a significantly greater hyperfine field. The differences between various combinations of the four hyperfine fields show maxima at about 10 K. At 1.14 K the field values are 540, 529, 519, and 509 kOe. The isomer shifts for each site are similar at ca. 0.52 mm/s, and the quadrupole shifts are small at ca. ±0.01 mm/s. Magnetic susceptibility studies confirm that the material is paramagnetic above ca. 20 K, with an effective magnetic moment of 5.92 μ_B and a Curie–Weiss temperature of −55.6 K. The magnetic susceptibility shows a peak of ca. 10 K, the magnitude of which increases with decreasing applied field between 45.81 and 9.95 kG. The magnetization data also indicate spontaneous ferrimagnetic ordering for iron(III) molybdate below ca. 14 K with a maximum in the spontaneous moment between 9 and 10 K. This behavior confirms that, below ca. 20 K, iron(III) molybdate is a weak L-type ferrimagnet. At temperatures below 6 K, the magnetic susceptibility increases at high applied fields, indicating the presence of a spin–flop transition with a critical field of ca. 20 kG at 4.2 K.

Introduction

We have previously published[2] a study of monoclinic, anhydrous iron(III) sulfate, $Fe_2(SO_4)_3$, which shows novel ferrimagnetic ordering arising from the presence of two crystallographically distinct octahedral iron(III) sites. The results provided a prescription for identifying materials with similar properties, and we have now completed a detailed investigation of the magnetic properties of the structurally related iron(III) molybdate, $Fe_2(MoO_4)_3$.

Iron(III) molybdate is chemically isostructural with iron(III) sulfate,[2,3] the structure consisting of an infinite network of iron–oxygen–molybdenum linkages in which the oxygen atoms coordinate the iron atoms octahedrally and the molybdenum atoms tetrahedrally; the octahedra share corners with the tetrahedra. However, there is an important crystallographic difference between the structures in that there are either four[3] or eight[4] distinct iron(III) sites in the molybdate and the unit cell has twice the volume of that of the sulfate, which contains only two iron(III) sites. The structure of the molybdate, as determined by Chen,[3] is presented in Figure 1. The uncertainty concerning the number of iron(III) sites arises because

(1) (a) Inorganic Chemistry Laboratory, Oxford University. (b) Chemical Crystallography Laboratory, Oxford University. (c) University of Missouri—Rolla. Address correspondence to G.J.L. at this address. (d) Atomic Energy Research Establishment.
(2) Long, G. J.; Longworth, G.; Battle, P.; Cheetham, A. K.; Thundathil, R. V.; Beveridge, D. *Inorg. Chem.* **1979**, *18*, 624.
(3) Chen, H. *Mater. Res. Bull.* **1979**, *14*, 1583.
(4) Rapposch, M. H.; Anderson, J. B.; Kostiner, E. *Inorg. Chem.* **1980**, *19*, 3531.

0020-1669/82/1321-4223$01.25/0